LETTERS

Template-directed synthesis of a genetic polymer in a model protocell

Sheref S. Mansy[1], Jason P. Schrum[1], Mathangi Krishnamurthy[1], Sylvia Tobé[1], Douglas A. Treco[1] & Jack W. Szostak[1]

Contemporary phospholipid-based cell membranes are formidable barriers to the uptake of polar and charged molecules ranging from metal ions to complex nutrients. Modern cells therefore require sophisticated protein channels and pumps to mediate the exchange of molecules with their environment. The strong barrier function of membranes has made it difficult to understand the origin of cellular life and has been thought to preclude a heterotrophic lifestyle for primitive cells. Although nucleotides can cross dimyristoyl phosphatidylcholine membranes through defects formed at the gel-to-liquid transition temperature[1,2], phospholipid membranes lack the dynamic properties required for membrane growth. Fatty acids and their corresponding alcohols and glycerol monoesters are attractive candidates for the components of protocell membranes because they are simple amphiphiles that form bilayer membrane vesicles[3–5] that retain encapsulated oligonucleotides[3,6] and are capable of growth and division[7–9]. Here we show that such membranes allow the passage of charged molecules such as nucleotides, so that activated nucleotides added to the outside of a model protocell spontaneously cross the membrane and take part in efficient template copying in the protocell interior. The permeability properties of prebiotically plausible membranes suggest that primitive protocells could have acquired complex nutrients from their environment in the absence of any macromolecular transport machinery; that is, they could have been obligate heterotrophs.

Previous observations of the slow permeation of UMP across fatty-acid-based membranes[6] stimulated us to explore the structural factors that control the permeability of these membranes (Fig. 1). We examined membrane compositions with varied surface charge density, fluidity, and stability of regions of high local curvature. We began by studying the permeability of ribose, because this sugar is a key building block of the nucleic acid RNA, and because sugar permeability is conveniently measured with a real-time fluorescence readout of vesicle volume after solute addition[10,11]. We used pure myristoleic acid (C14:1 fatty acid, myristoleate in its ionized form) as a reference composition, because this compound generates robust vesicles that are more permeable to solutes than the more common longer chain oleic acid. Both myristoleyl alcohol and the glycerol monoester of myristoleic acid (monomyristolein, GMM) stabilize myristoleate vesicles to the disruptive effects of divalent cations[3,6]. Addition of these amphiphiles should decrease the surface charge density of myristoleate vesicles, whereas myristoleyl phosphate should increase the surface charge density. Surprisingly, only the addition of GMM affected ribose permeability, leading to a fourfold increase (Fig. 2a). This result suggested that surface charge density *per se* was not a major factor controlling sugar permeability.

We hypothesized that the larger steric bulk of the glycerol-ester head group of GMM relative to the carboxylate of myristoleic acid might increase ribose permeability by stabilizing highly curved surfaces associated with the formation of transient solute–lipid complexes[12]. We therefore examined the effect of the glycerol esters of the longer chain amphiphiles palmitoleic acid (C16:1) and oleic acid (C18:1) on the permeability of pure palmitoleic acid and oleic acid membranes. These molecules, which are progressively less cone-shaped than GMM, had an increasingly smaller influence on the permeability of the corresponding pure fatty acid membranes (Fig. 2b). However, the addition of sorbitan monooleate, which has a larger cyclic 6-carbon sugar head group (thus restoring a more conical shape to this 18-carbon fatty acid), resulted in a fourfold increase in the permeability of oleic acid membranes, consistent with the hypothesis that cone-shaped amphiphiles stabilize highly curved membrane deformations that facilitate solute passage. Decreasing acyl chain length within a series of homologous fatty acids (or mixtures of fatty acids and their glycerol esters) also led to increased sugar

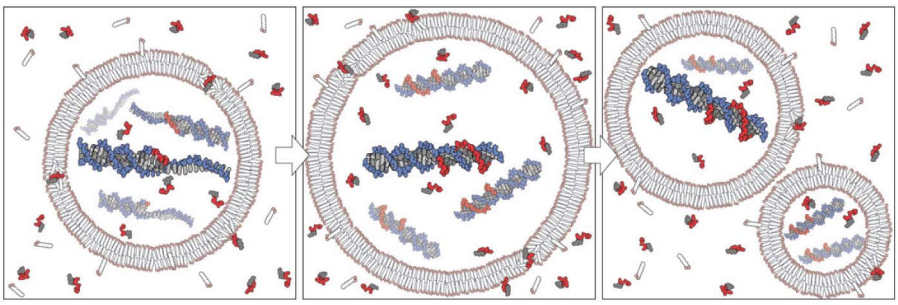

Figure 1 | Conceptual model of a heterotrophic protocell. Growth of the protocell membrane results from the incorporation of environmentally supplied amphiphiles, whereas division may be driven by intrinsic or extrinsic physical forces. Externally supplied activated nucleotides permeate across the protocell membrane and act as substrates for the non-enzymatic copying of internal templates. Complete template replication followed by random segregation of the replicated genetic material leads to the formation of daughter protocells.

[1]Howard Hughes Medical Institute, Department of Molecular Biology and the Center for Computational and Integrative Biology, Massachusetts General Hospital, Boston, Massachusetts 02114, USA.

permeability (Fig. 2b and Supplementary Table 1), presumably owing to the decreased stability of the ideal bilayer structure with respect to the formation of transient solute–lipid complexes.

To investigate further the idea that local membrane deformations are required for solute passage across the membrane, we asked whether increased packing disorder within the lipid bilayer would enhance permeability. Phospholipids with higher degrees of unsaturation yield more disordered, fluid membranes that are more permeable to water and small solutes[13]. We observed a fivefold increase in ribose permeability for vesicles composed of linoleic acid (C18:2) versus oleic acid (C18:1). Branched-chain amphiphiles such as the isoprenoid farnesol also increase the fluidity of phospholipid membranes[14]. Vesicles made from a 2:1 molar mixture of myristoleic acid and farnesol exhibited a ~17-fold increase in ribose permeability relative to pure myristoleic acid vesicles. Conversely, the higher packing density of saturated amphiphiles[13] should lead to increased membrane order and decreased solute permeability. As expected, the addition of lauric acid (C12:0) to myristoleic acid vesicles (2:1 myristoleic acid:lauric acid) resulted in a twofold decrease in ribose permeability (Fig. 2c).

The above experiments show that solute permeability can be increased by decreasing acyl chain length, by increasing acyl chain unsaturation or branching, and by adding amphiphiles with larger head groups. The most prebiotically plausible amphiphiles are the short chain saturated fatty acids and their corresponding alcohols and glycerol esters[15–17]. To see whether shorter chain length could compensate for the loss of unsaturation, we tested membrane compositions based on the C10 amphiphiles decanoic acid and decanol (DOH) as well as the glycerol monoester of decanoate (GMD). Pure decanoic acid only forms stable vesicles at very high amphiphile concentrations (≥100 mM), but the addition of decanol decreases the critical aggregate concentration to ~20 mM and increases the pH range over which vesicles are stable[3]. We found that the ribose permeability of 2:1 decanoate:decanol vesicles is very similar to that of myristoleic acid vesicles but is significantly less than that of myristoleic acid:GMM vesicles (Fig. 2d). Based on the observations that amphiphiles with larger head groups lead to increased permeability, we replaced half of the decanol with glycerol mono-decanoate. The resulting vesicles exhibited a tenfold increase in ribose permeability (Fig. 2d). It is particularly notable that improved permeability and stability are obtained with mixtures of amphiphiles, such as might be expected to be present in a chemically rich prebiotic environment. This is in marked contrast to the situation with nucleic acids, where homogeneous nucleotides are thought to be required for replication.

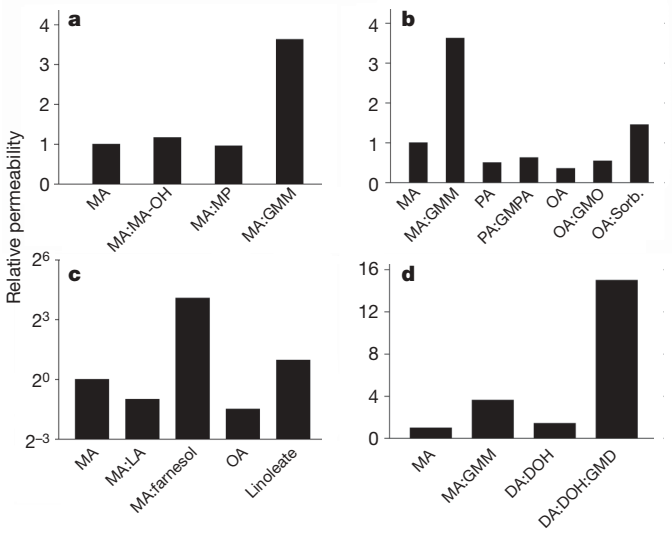

Figure 2 | Ribose permeability of fatty acid based membranes. **a–c**, Influence of head group charge (**a**), head group size (**b**) and membrane fluidity (**c**). **d**, Comparison of decanoic-acid-based membranes with myristoleic acid based membranes. All binary lipid mixtures were 2:1 molar ratios of fatty acid:additive; a 4:1:1 ratio of decanoic acid:DOH:GMD was used. Ribose permeabilities are relative to that of myristoleic acid membranes. DA, decanoic acid; DOH, decanol; GMD, glycerol monoester of decanoic acid; GMM, glycerol monoester of myristoleate; GMO, glycerol monoester of oleate; GMPA, glycerol monoester of palmitoleate; LA, lauric acid; MA, myristoleic acid; MA-OH, myristoleoyl alcohol; MP, myristoleoyl phosphate; OA, oleate; PA, palmitoleic acid; Sorb., sorbitan monooleate.

Vesicles with all of the above membrane compositions retained 100% of an encapsulated fluorescein-labelled dA_{10} oligonucleotide indefinitely (Supplementary Fig. 6). In addition, all membrane compositions retained the previously observed 3–10-fold faster permeation of ribose compared to its diastereomers arabinose, lyxose and xylose (Supplementary Table 1). These observations show that our permeability measurements do not reflect leakage of encapsulated materials caused by vesicle rupture or the formation of large non-selective pores.

Having established that membranes composed of prebiotically plausible amphiphilic molecules have high permeabilities to simple sugars, we asked whether such membranes would allow the uptake of nucleotide nutrients by a simple model protocell. We measured nucleotide permeation by encapsulating nucleotides within vesicles and then determining the fraction of the encapsulated nucleotide that had leaked out of the vesicles at various times. Because charge has such a dominant effect in restricting solute permeation through membranes, we first examined the effect of nucleotide charge on permeation through myristoleic acid:GMM (2:1) membranes. We observed negligible leakage of AMP, ADP or ATP (with 2, 3 and 4 negative charges at pH 8.5, respectively) over 24 h in the absence of Mg^{2+}, suggesting that these molecules were either too large or too highly charged to cross the membrane. We did observe slow permeation of AMP and ADP in the presence of 3 mM Mg^{2+} (Fig. 3a), as expected from the formation of complexes of reduced net charge[18]. The impermeability of ATP argues against a role for NTPs in very early forms of cellular life dependent on externally synthesized activated nucleotides; instead, NTPs may be a later evolutionary adaptation that prevents the leakage of internally synthesized activated nucleotides[19].

The above results highlight the importance of reducing the net charge of nucleotides to enhance membrane permeability. Imidazole-activated nucleotides have been used as convenient models of prebiotic activated nucleotides in studies of both spontaneous and templated polymerization reactions[20–23]. In addition to their higher intrinsic chemical reactivity compared to NTPs, these activated nucleotides are less polar and bear only a single negative charge at a neutral to moderately alkaline pH. We therefore measured the permeabilities of a series of adenosine nucleotides and their corresponding phosphorimidazolides, using both myristoleic acid:GMM (2:1) and C10 membranes (4:1:1 decanoic acid:DOH:GMD; Fig. 3b–d). The half-time for equilibration of nucleoside phosphorimidazolides using 100-nm vesicles was approximately 12 h. The effects of membrane composition on the permeability of nucleoside phosphorimidazolides were essentially parallel to our results for sugar permeability—pure myristoleic acid vesicles were less permeable to nucleotides than myristoleic acid:GMM (2:1) vesicles, whereas farnesol led to an even greater enhancement of permeability (Supplementary Fig. 4). Similarly, the permeability of decanoic acid:DOH membranes was enhanced by the addition of GMD (Fig. 3d).

Our permeability data are consistent with a transport model in which polar functional groups of solute molecules initially interact with one or more amphiphile head groups with displacement of bound water molecules (Supplementary Fig. 5), whereas non-polar regions of the solute may interact with the hydrophobic acyl chains of the amphiphiles[24]. Formation of this relatively non-specific amphiphile–solute complex is followed by a concerted inversion of the complex across the membrane. Lipids with large head groups could increase solute permeation by providing more opportunity for solute

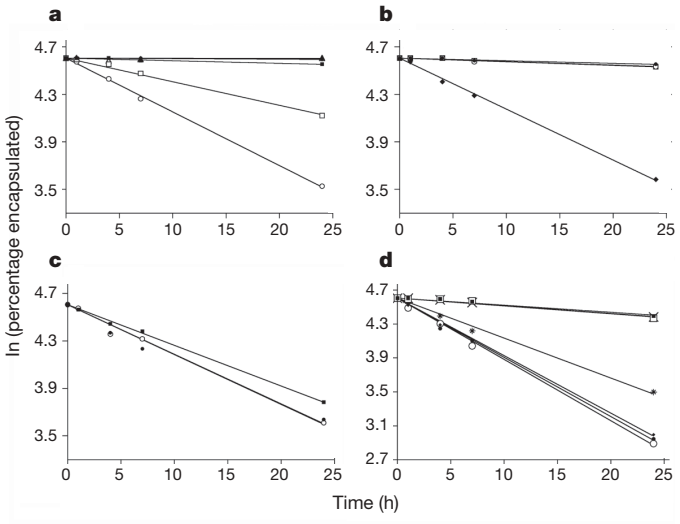

Figure 3 | Time courses of nucleotide permeation through fatty acid based membranes. **a**, Nucleotide permeation across MA:GMM membranes. Filled square, AMP; open square, AMP + 3 mM $MgCl_2$; filled circle, ADP; open circle, ADP + 3 mM $MgCl_2$, filled triangle, ATP; open triangle, ATP + 3 mM $MgCl_2$. **b**, Permeation of AMP derivatives across MA:GMM membranes. Filled circle, adenosine-5′-monophosphate; open circle, 2′-deoxyadenosine-5′-monophosphate; open square, 2′-amino-2′,3′-dideoxyadenosine-5′-monophosphate; filled diamond, 2′-deoxyadenosine-5′-phosphorimidazolide. **c**, Permeability of activated nucleotides across MA:GMM membranes. Filled square, adenosine-5′-phosphorimidazolide; filled circle, 2′-amino-2′,3′-dideoxyadenosine-5′-phosphorimidazolide; open circle, 3′-amino-3′-deoxyadenosine-5′-phosphorimidazolide. **d**, Nucleotide permeation across DA:DOH:GMD and DA:DOH membranes. Filled square, AMP; open square, dAMP; X, 2′-amino-2′,3′-dideoxyadenosine-5′-monophosphate; filled diamond and asterisk, adenosine-5′-phosphorimidazolide; filled circle, 2'-deoxyadenosine-5′-phosphorimidazolide; open circle, 2′-amino-2′,3′-dideoxyadenosine-5′-phosphorimidazolide. All are for 4:1:1 DA:DOH:GMD membranes except for the asterisk, which is 2:1 DA:DOH.

interaction, by favouring high local curvature and by decreasing the cohesive interactions between adjacent acyl chains and thereby facilitating amphiphile flip-flop. This model is similar to the previously proposed carrier model for the spontaneous transport of monovalent ions across fatty acid[25] and phospholipid membranes[26].

Encouraged by the observed permeability of activated nucleotides, we asked whether such nucleotides added to the outside of a model protocell could diffuse to the inside and engage in template-copying reactions in the vesicle interior. Although no sequence-general means for the non-enzymatic replication of a genetic polymer has yet been found, we have identified a system that exhibits remarkably rapid and efficient non-enzymatic copying of an oligo-dC DNA template (Supplementary Fig. 7). We used this system to model the spontaneous chemical replication of genetic material within a protocell. In brief, a DNA primer bearing a single 3′-amino-nucleotide at its 3′ terminus[27] was annealed to a DNA oligonucleotide consisting of a primer-binding region and a $(dC)_{15}$ template region. After the addition of 2′-amino, 2′-3′-dideoxyguanosine 5′-phosphorimidazolide, the primer was extended by the template-directed synthesis of 2′-phosphoramidate-linked DNA. Both 3′- and 2′-amino nucleotides polymerized much more rapidly than similarly activated ribo- or deoxyribo-nucleotides owing to the presence of the more nucleophilic amino group[23]. In solution, primer-extension across a $(dC)_{15}$ template in the presence of 5 mM activated 2′-amino-guanosine is essentially complete within 6 h (Fig. 4a). The principal product is full-length extended primer.

We used the reaction described previously to test the chemical and physical compatibility of template-directed copying with the integrity of fatty-acid-based vesicles. We examined the same template-copying reaction inside two sets of vesicles: the robust laboratory model system consisting of myristoleic acid:GMM (2:1) vesicles, and the more prebiotically plausible decanoic acid:DOH:GMD (4:1:1) vesicles. Vesicles containing encapsulated primer-template were purified to remove unencapsulated primer-template. We added 5 mM activated 2′-amino-guanosine to initiate template copying, removed aliquots at intervals, and again purified the vesicles to remove traces of primer-template that might have leaked out of the vesicles. The absence of measurable leakage of oligonucleotides from the vesicles shows that the activated nucleotides do not disrupt vesicle structure. Analysis of the reaction products showed significant primer-extension by 3 h, with full-length product continuing to accumulate until 24 h, at which point the vesicle reactions had reached a level of full-length product comparable to that seen in the solution reactions (Fig. 4). Thus, myristoleic acid:GMM or decanoic acid:DOH:GMD membranes slow the interaction between the primer-template and activated nucleotides, but are nevertheless compatible with template-copying chemistry in the vesicle interior. As expected, a similar experiment using myristoleic acid:farnesol (2:1) vesicles also showed efficient copying of encapsulated template (Fig. 4c). In contrast, phospholipid vesicles showed no detectable primer extension after the addition of activated nucleotide to the vesicle exterior (Fig. 4d).

The results described above bear directly on the two current contrasting views of the nature of protocells: the autotrophic and

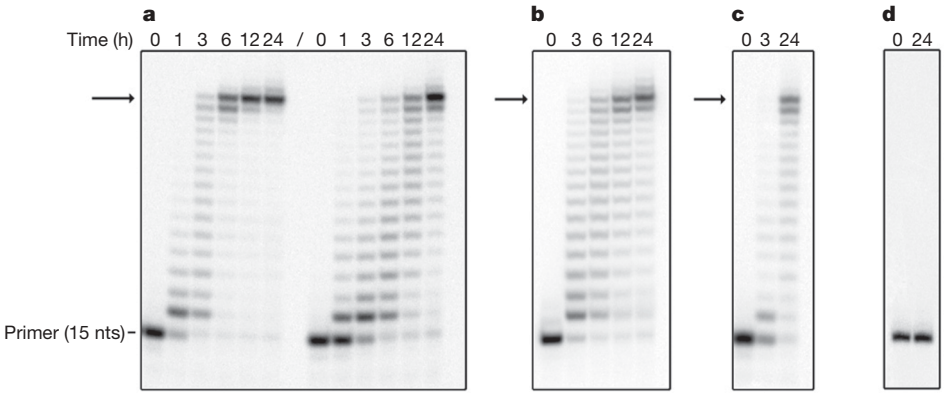

Figure 4 | Template-copying chemistry inside vesicles. Vesicles contained encapsulated primer-template complexes, and template-copying was initiated by the addition of activated monomer to the external solution. nts, nucleotides. **a**, Non-enzymatic dC_{15}-template copying in solution (lanes 1–6) and inside 2:1 MA:GMM vesicles (lanes 8–13) at 4 °C. **b**, Template-copying reaction in 4:1:1 DA:DOH:GMD vesicles at 25 °C. **c**, Template-copying reaction in 2:1 MA:farnesol vesicles at 4 °C. **d**, Template-copying reaction in POPC vesicles at 4 °C. For **a**–**c**, the arrow denotes full-length product. See Methods for reaction conditions.

heterotrophic models[28–30]. The autotrophic or 'metabolism first' model is based on the idea that autocatalytic reaction networks evolved in a spatially localized manner to generate *in situ* the building blocks required for cellular replication. Our results argue that early protocells with fatty-acid-based membranes could not have been autotrophs, because internally generated metabolites would leak out. In contrast, the heterotrophic model posits the emergence of very simple cellular structures within a complex environment that provides external sources of nutrients and energy. Although both models must overcome numerous conceptual difficulties related to the origin of complex molecular building blocks, the heterotrophic model was thought to face the additional difficulty of importing polar and even charged molecules across a bilayer lipid membrane. We have shown that fatty-acid-based membranes allow a simple protocell to acquire critical nutrients, while retaining polymerized nucleic acids indefinitely. Our results therefore support the idea that extremely simple heterotrophic protocells could have emerged within a prebiotic environment rich in complex nutrients.

METHODS SUMMARY

Sugar permeability. Vesicles were prepared with 10 mM encapsulated calcein in either 0.1 M POPSO (piperazine-1,4-bis(2-hydroxypropanesulfonic acid) dihydrate) and 3 mM EDTA (pH 8.2) or 0.1 M POPSO and 3 mM $MgCl_2$ (pH 8.2). Final sugar concentrations were either 0.5 M or 0.1 M. Permeability was measured by the shrink–swell assay[11] on an Applied Photophysics SX.18MV-R stopped-flow spectrometer at 23 °C.

Nucleotide permeability. Nucleotide permeability measurements were in 0.2 M sodium bicine (pH 8.5) at 23 °C and measured either by monitoring the leakage of entrapped nucleotide by radioactivity or by ultraviolet absorption. Separation of vesicle-entrapped and -released nucleotide was by gel filtration.

Primer extension reactions. Reactions contained 0.1 μM ^{32}P-labelled 3′-amino-terminated primer, 0.5 μM template DNA, 100 mM 1-(2-hydroxyethyl)-imidazole and 200 mM sodium bicine (pH 8.5). Reactions were initiated by the addition of 5 mM 2′-amino-2′,3′-dideoxyguanosine-5′-phosphorimidazolide and incubated at 4 °C. Samples were analysed by electrophoresis on a denaturing 17% polyacrylamide gel. Reaction products were visualized using a Typhoon 9410 PhosphorImager.

Full Methods and any associated references are available in the online version of the paper at www.nature.com/nature.

Received 29 October 2007; accepted 22 April 2008.
Published online 4 June 2008.

1. Chakrabarti, A. C., Breaker, R. R., Joyce, G. F. & Deamer, D. W. Production of RNA by a polymerase protein encapsulated within phospholipid vesicles. *J. Mol. Evol.* **39,** 555–559 (1994).
2. Monnard, P. A., Luptak, A. & Deamer, D. W. Models of primitive cellular life: polymerases and templates in liposomes. *Phil. Trans. R. Soc. Lond. B* **362,** 1741–1750 (2007).
3. Apel, C. L., Deamer, D. W. & Mautner, M. N. Self-assembled vesicles of monocarboxylic acids and alcohols: conditions for stability and for the encapsulation of biopolymers. *Biochim. Biophys. Acta* **1559,** 1–9 (2002).
4. Blochliger, E., Blocher, M., Walde, P. & Luisi, P. L. Matrix effect in the size distribution of fatty acid vesicles. *J. Phys. Chem. B* **102,** 10383–10390 (1998).
5. Hargreaves, W. R. & Deamer, D. W. Liposomes from ionic, single-chain amphiphiles. *Biochemistry* **17,** 3759–3768 (1978).
6. Chen, I. A., Salehi-Ashtiani, K. & Szostak, J. W. RNA catalysis in model protocell vesicles. *J. Am. Chem. Soc.* **127,** 13213–13219 (2005).
7. Chen, I. A., Roberts, R. W. & Szostak, J. W. The emergence of competition between model protocells. *Science* **305,** 1474–1476 (2004).
8. Chen, I. A. & Szostak, J. W. A kinetic study of the growth of fatty acid vesicles. *Biophys. J.* **87,** 988–998 (2004).
9. Hanczyc, M. M., Fujikawa, S. M. & Szostak, J. W. Experimental models of primitive cellular compartments: encapsulation, growth, and division. *Science* **302,** 618–622 (2003).
10. Chen, P. Y., Pearce, D. & Verkman, A. S. Membrane water and solute permeability determined quantitatively by self-quenching of an entrapped fluorophore. *Biochemistry* **27,** 5713–5718 (1988).
11. Sacerdote, M. G. & Szostak, J. W. Semipermeable lipid bilayers exhibit diastereoselectivity favoring ribose. *Proc. Natl Acad. Sci. USA* **102,** 6004–6008 (2005).
12. Israelachvili, J. N. *Intermolecular and Surface Forces* (Academic, London, 1992).
13. Lande, M. B., Donovan, J. M. & Zeidel, M. L. The relationship between membrane fluidity and permeabilities to water, solutes, ammonia, and protons. *J. Gen. Physiol.* **106,** 67–84 (1995).
14. Rowat, A. C., Keller, D. & Ipsen, J. H. Effects of farnesol on the physical properties of DMPC membranes. *Biochim. Biophys. Acta* **1713,** 29–39 (2005).
15. Deamer, D. W. Boundary structures are formed by organic components of the Murchison carbonaceous chondrite. *Nature* **317,** 792–794 (1985).
16. Huang, Y. *et al.* Molecular and compound-specific isotopic characterization of monocarboxylic acids in carbonaceous meteorites. *Geochim. Cosmochim. Acta* **69,** 1073–1084 (2005).
17. McCollom, T. M., Ritter, G. & Simoneit, B. R. Lipid synthesis under hydrothermal conditions by Fischer–Tropsch-type reactions. *Orig. Life Evol. Biosph.* **29,** 153–156 (1999).
18. Khalil, M. M. Complexation equilibria and determination of stability constants of binary and ternary complexes with ribonucleotides (AMP, ADP, and ATP) and salicylhydroxamic acid as ligands. *J. Chem. Eng. Data* **45,** 70–74 (2000).
19. Westheimer, F. H. Why nature chose phosphates. *Science* **235,** 1173–1178 (1987).
20. Eschenmoser, A. The search for the chemistry of life's orgin. *Tetrahedron* **63,** 12821–12844 (2007).
21. Ferris, J. P., Hill, A. R., Liu, R. & Orgel, L. E. Synthesis of long prebiotic oligomers on mineral surfaces. *Nature* **381,** 59–61 (1996).
22. Kozlov, I. A., Pitsch, S. & Orgel, L. E. Oligomerization of activated D- and L-guanosine mononucleotides on templates containing D- and L-deoxycytidylate residues. *Proc. Natl Acad. Sci. USA* **95,** 13448–13452 (1998).
23. Tohidi, M., Zielinski, W. S., Chen, C. H. & Orgel, L. E. Oligomerization of the 3′-amino-3′deoxyguanosine-5′phosphorimidazolidate on a d(CpCpCpCpC) template. *J. Mol. Evol.* **25,** 97–99 (1987).
24. Wilson, M. A. & Pohorille, A. Mechanism of unassisted ion transport across membrane bilayers. *J. Am. Chem. Soc.* **118,** 6580–6587 (1996).
25. Chen, I. A. & Szostak, J. W. Membrane growth can generate a transmembrane pH gradient in fatty acid vesicles. *Proc. Natl Acad. Sci. USA* **101,** 7965–7970 (2004).
26. Paula, S. G., Volkov, A. G., Van Hoek, A. N., Haines, T. H. & Deamer, D. W. Permeation of protons, potassium ions, and small polar molecules through phospholipid bilayers as a function of membrane thickness. *Biophys. J.* **70,** 339–348 (1996).
27. Hagenbuch, P., Kervio, E., Hochgesand, A., Plutowski, U. & Clemens, R. Chemical primer extension: efficiently determining single nucleotides in DNA. *Angew. Chem. Int. Edn Engl.* **44,** 6588–6592 (2005).
28. Chen, I. A., Hanczyc, M. M., Sazani, P. L. & Szostak, J. W. in *The RNA World* (eds Gesteland, R. F., Cech, T. R. & Atkins, J. F.) 57–88 (Cold Spring Harbor Laboratory Press, Cold Spring Harbor, 2006).
29. Morowitz, H. J. *Beginnings of Cellular Life: Metabolism Recapitulates Biogenesis* (Yale Univ. Press, New Haven, 2004).
30. Wachtershauser, G. Evolution of the first metabolic cycles. *Proc. Natl Acad. Sci. USA* **87,** 200–204 (1990).

Supplementary Information is linked to the online version of the paper at www.nature.com/nature.

Acknowledgements This work was supported by grants from the NASA Exobiology Program (EXB02-0031-0018) and the NSF (CHE-0434507) to J.W.S. J.W.S. is an Investigator of the Howard Hughes Medical Institute. S.S.M. was supported by the NIH (F32 GM07450601). We thank I. Chen, M. Hanczyc, R. Bruckner, T. Zhu and Q. Dufton for discussions, and J. Iwasa for Fig. 1 and Supplementary Fig. 5.

Author Contributions Permeability experiments were performed by S.S.M. J.P.S. performed primer-extension experiments. M.K. synthesized 2′-aminoguanosine. S.T. and D.A.T. contributed to the development of the encapsulated primer-extension system. All authors helped to design the experiments and discussed the results. S.S.M., J.P.S. and J.W.S. wrote the paper.

Author Information Reprints and permissions information is available at www.nature.com/reprints. Correspondence and requests for materials should be addressed to J.W.S. (szostak@molbio.mgh.harvard.edu).

METHODS

Materials. Fatty acids, fatty alcohols and the glycerol monoesters of fatty acids were obtained from Nu-chek Prep, Inc. POPC (1-palmitoyl-2-oleoyl-*sn*-glycero-3-phosphocholine) was from Avanti Polar Lipids, Inc. Myristoleoyl phosphate[31–33] was synthesized as described previously. 2′-amino-2′,3′-dideoxyguanosine-5′-phosphorimidazolide was synthesized by first generating 2′-azido-2′,3′-dideoxyguanosine, as described previously [34], followed by phosphorylation of the 2′-azido-2′,3′-dideoxy nucleoside with $POCl_3$ in triethyl phosphate, activation with 1,1′-carbonyl-diimidazole (CDI) to yield the 5′-phosphorimidazolide, and reduction of the 2′-azido group to the 2′-amine by catalytic hydrogenation. Nucleotide phosphorimidazolides were then purified by reverse-phase HPLC on an Alltima C18 column (Alltech) equilibrated with 0.1 M triethylammonium bicarbonate/2% acetonitrile, pH 8.0, and eluted with an acetonitrile gradient. Oligonucleotides were synthesized on an Expedite 8909 DNA synthesizer (Applied Biosystems). Template DNA (5′-AACCCCCCC CCCCCCCCCCAGTCAGTCTACGC-3′) for primer extension reactions was synthesized using standard phosphoramidite chemistry. 3′-amino-terminated DNA primer (5′-GCGTAGACTGACTGG-NH_2-3′) was synthesized using reverse phosphoramidites (Glen Research), with the final addition using a 3′-amino phosphoramidite (Transgenomic). Oligonucleotides were purified by anion exchange HPLC on a DNAPac PA-100 column (Dionex) in 0.01 M NaOH/0.01 M NaCl, pH 12.0, in a gradient up to 1.5 M NaCl.

Vesicle preparation. Fatty acid vesicles were prepared by oil dispersion in buffered solutions as described previously[1,3]. For vesicles composed of mixtures of unsaturated amphiphiles, the oils were mixed before dispersion in aqueous solution. Vesicles of mixed saturated and unsaturated composition were made by first generating vesicles composed of the unsaturated amphiphile, extrusion through 100 nm pore-size polycarbonate filters, followed by the addition of micelles composed of the saturated fatty acid. All vesicle preparations were extruded 11 times with an Avanti mini-extruder. For the encapsulation of molecules, amphiphiles were resuspended in the presence of the encapsulant followed by freeze-thaw cycling to equilibrate internal and external solutes. Separation of entrapped and unencapsulated material was by gel filtration with Sepharose-4B resin (Sigma-Aldrich) in which the running buffer contained the same amphiphile composition as the vesicles at a concentration above their critical aggregate concentration. Vesicle size was measured by dynamic light scattering with a PDDLS/CoolBatch 90T from Precision Detectors.

Sugar permeability. Vesicles were prepared with 10 mM encapsulated calcein in either 0.1 M POPSO and 3 mM EDTA, pH 8.2, or 0.1 M POPSO and 3 mM $MgCl_2$, pH 8.2. Final sugar concentrations were either 0.5 M or 0.1 M. Before measurement, vesicle samples were diluted to 4 mM amphiphile in buffer containing amphiphiles of equivalent composition as the vesicle above its critical aggregate concentration (myristoleic-acid-containing vesicles, 4 mM; palmitoleic-acid-containing vesicles, 1 mM; oleic-acid-containing vesicles, 0.1 mM; decanoic-acid-containing vesicles, 20 mM). Permeability was measured by the shrink–swell assay[13] on an Applied Photophysics SX.18MV-R stopped-flow spectrometer at 23 °C. The rate of the initial volume decrease due to water efflux yields the water permeability P_w, and the rate of the slower relaxation back to the initial volume reflects solute entry and yields the solute permeability P_s. Excitation and emission were at 470 nm and 540–560 nm, respectively. To avoid inner-filter effects and interferences arising from scattered light, all samples had absorbance values at 470 nm and 600 nm < 0.1. Size-exclusion chromatography showed that no calcein leaked out of the vesicles during the stopped-flow experiments.

Nucleotide permeability. Nucleotide permeability measurements were in 0.2 M sodium bicine, pH 8.5, at 23 °C and were measured either by monitoring the leakage of entrapped nucleotide by radioactivity or by ultraviolet absorption. The leakage of radioactive nucleotide was measured by loading aliquots at different time points on a gel filtration column and analysing fractions by scintillation counting. Permeability measurements of non-radioactive nucleotides were similarly performed, except that quantification relied on 260 nm absorbance following twofold dilution of the fractions with methanol.

Primer extension reactions. Reactions contained 0.1 μM ^{32}P-labelled 3′-amino-terminated primer, 0.5 μM template DNA, 100 mM 1-(2-hydroxyethyl)-imidazole, and 200 mM sodium bicine, pH 8.5. Reactions were initiated by the addition of 5 mM 2′-amino-2′,3′-dideoxyguanosine-5′-phosphorimidazolide and incubated at 4 °C. Solution reactions were stopped by adding three volumes formamide and heating to 95 °C for 10 min followed by ethanol precipitation. Vesicle reactions were stopped by gel filtration followed immediately by the addition of 0.3% Triton X-100 and ethanol precipitation. Stopped reactions were then resuspended in formamide gel loading buffer and heated to 95 °C for 2 min. Samples were analysed by electrophoresis on a denaturing 17% polyacrylamide gel. Reaction products were visualized using a Typhoon 9410 PhosphorImager. 1-(2-hydroxyethyl)imidazole enhances both non-enzymatic polymerization and nucleotide permeability by about twofold without affecting membrane integrity (Supplementary Figs 2 and 3). We confirmed that the primer was extended with phosphoramidate-linked G residues by the expected sensitivity to acid hydrolysis; in separate experiments with a shorter primer and template, we confirmed the non-enzymatic synthesis of phosphoramidate linked DNA by matrix assisted laser desorption/ionization time of flight mass spectrometry (MALDI-TOF-MS).

Vesicle stability. The stability of vesicles of different compositions was assessed by quantifying leakage of entrapped 5′-fluorescein-labelled dA_{10} (Massachusetts General Hospital DNA Core Facility) after 24 h at 23 °C in 0.2 M sodium bicine, pH 8.5. Vesicles were separated from leaked oligonucleotides by gel filtration chromatography (Sepharose 4B) and quantified by fluorescence ($\lambda^{excitation} = 490$ nm, $\lambda^{emission} = 520$ nm) with a SpectraMAX GeminiEM fluorescence plate reader (Molecular Devices). To test the influence of 1-(2-hydroxyethyl)imidazole on vesicle stability, 2:1 myristoleic acid:GMM vesicle solutions were supplemented with 100 mM 1-(2-hydroxyethyl)imidazole and tested as described previously.

31. Danilov, L. L. & Chojnacki, T. A simple procedure for preparing dolichyl monophosphate by the use of $POCl_3$. *FEBS Lett.* **131,** 310–312 (1981).
32. Guernelli, S. *et al.* Supramolecular complex formation: a study of the interactions between β-cyclodextrin and some different classes of organic compounds by ESI-MS, surface tension measurements, and UV/Vis and ^{1}H NMR spectroscopy. *Eur. J. Org. Chem.* **24,** 4765–4776 (2003).
33. Nelson, A. K. & Toy, A. D. F. The preparation of long-chain monoalkyl phosphates from pyrophosphoric acid and alcohols. *Inorg. Chem.* **2,** 775–777 (1963).
34. Kawana, M. & Kuzuhara, H. General method for the synthesis of 2′-azido-2′,3′-dideoxynucleosides by the use of [1,2]-hydride shift and β-elimination reactions. *J. Chem. Soc. Perkin Trans. I* **4,** 469–478 (1992).